Selective Electrochemical Ammonia Production via Electron-Limiting Catalytic Devices

Investigators

Stacey F. Bent, Professor, Chemical Engineering; Bruce Clemens, Professor, Materials Science and Engineering; Jon Baker, Melissa Wette, Graduate Researchers, Stanford University

Abstract

Electrochemical production of ammonia is a booming area of research for good reason – while the problem is hard, the potential impact is huge. One of the chief difficulties of realizing this technology is the extremely low selectivity of the key electrochemical reaction that reduces nitrogen from its gaseous state. In this research, we designed a catalyst-insulator-metal device to improve the efficiency of the nitrogen reduction reaction by interfering with its chief competitor, the hydrogen evolution reaction (HER). This interference was achieved by modulating electron availability through an atomic layer deposited (ALD) tunneling barrier oxide. We successfully established HER suppression with increasing insulator thickness. Furthermore, we developed an inert gas condensation synthesis for the catalyst nanoparticles, and demonstrated strategies for improving adhesion at the catalyst-insulator interface.

Introduction

Ammonia is an incredibly important chemical, thought to support half the world's population from the fertilizer in which it's used[1]. Currently, the Haber-Bosch process is used to produce this essential chemical, eating up 2% of the world's energy each year and producing 5% of all methane emissions in the process.[2,3] Innovation in this area thus represents a huge opportunity for greenhouse gas (GHG) emissions savings. In this project we aimed to tackle this problem by designing a device to electrochemically produce ammonia. This proposed device works by using a tunneling barrier to starve the competing hydrogen evolution reaction (HER) of electrons and thus improve the selectivity for ammonia. Such a device requires careful optimization of many component parts – development of a tunneling barrier with the appropriate electrical properties, incorporation of a catalyst with the requisite binding energy, demonstration of HER suppression as a function of insulator thickness, and amidst all this stability of all parts of the system under operating conditions. Herein we describe in detail our approach and contributions to the field of electrochemical ammonia production.

Background

Continuous nitrogen reduction by electrochemical means remains challenging due to poor selectivity over reduction of protons to hydrogen in aqueous electrolytes. While there have been a variety of reports in literature reporting ammonia production in aqueous media, these systems suffer from low rates and selectivity. In addition, such low amounts of ammonia produced call into question the potential of external ammonia contamination producing false positives.[4]

Progress has been made in improving selectivity for ammonia production using non-aqueous electrolytes, increasing selectivity to ammonia up to as high as 90%.[4,5-8] These electrochemical systems rely on improving selectivity by carefully controlling proton availability, effectively suppressing the hydrogen evolution reaction. These systems highlight the ability to electrochemically produce ammonia with proper suppression of the hydrogen evolution reaction. To date, limiting access to electrons to suppress the hydrogen evolution reaction over the nitrogen reduction reaction has yet to be studied. However, reports in literature of photocathodes which possess high selectivity to ammonia at low rates may indicate that control of electron availability can be used to improve selectivity.[9]

Results

ALD HfO_2 stability was tested under a variety of film deposition and electrolyte conditions. Deposition temperature was found to greatly influence stability under electrochemical conditions. At the lowest deposition temperature studied, T=100°C, films were found to etch in slightly acidic electrolyte (pH=4) and in alkaline electrolyte (pH=13). This was observed by film thickness decreases as measured by ellipsometry. Etching was enhanced when the films were electrochemically cycled, and resulted in increased removal of the as-deposited HfO_2. In addition, films deposited at 100°C were found unstable in phosphate buffer solution (PBS, pH=7) upon electrochemical cycling.

Increasing deposition temperature resulted in improved stability up to 200°C and remained stable up to 300°C. Films deposited between 200°C-300°C were found to be stable under electrochemical cycling in phosphate buffer solution (PBS) with pH=7. However, ALD HfO_2 deposited in this temperature range remained unstable at slightly acidic (pH=4) and alkaline electrolytes (pH=13). The improved stability is attributed to improved crystallinity of the film, where over this temperature range the films evolve from amorphous to polycrystalline.

With the new-found stability limits of ALD HfO_2, its tunneling barrier properties were investigated by cyclic voltammetry. ALD HfO_2 films deposited at 250°C on gold substrates were investigated in PBS with pH=7. Cyclic voltammetry of ALD HfO_2 films is shown in Figure 1. Reduction current is attributed to evolution of hydrogen ($2 H_2O + 2e^- \rightarrow H_2 + 2OH^-$). ALD HfO_2 resulted in suppressed hydrogen evolution current, with greater suppression with thicker films. However, conduction through the HfO_2 remained higher than expected for direct electron tunneling, indicating the presence of other conduction mechanisms, likely through mid-band gap states due to defects. The conduction of electrons through defects is undesirable, as the potential of the electrons will decrease as they travel through the barrier.
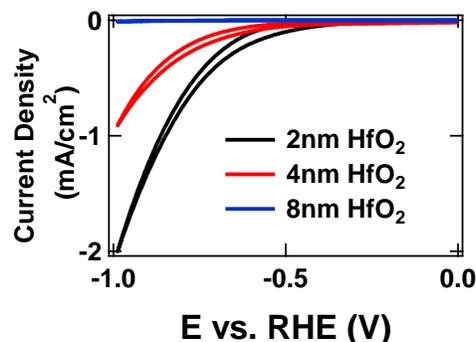
Figure 1: Cyclic voltammetry of ALD-HfO$_2$ ($T_{deposition}$=250°C) on gold substrates in PBS (pH=7). Different thicknesses are shown, current is attributed to evolution of hydrogen gas.

Addition of a second barrier, such as Al$_2$O$_3$ and SiO$_2$ was investigated. These metal oxides have large band gaps with suitable band positions, making them appropriate for tunneling barriers. However, Al$_2$O$_3$ and SiO$_2$ are prone to corrosion under the studied conditions. In this work, we found that capping Al$_2$O$_3$ and SiO$_2$ with ALD HfO$_2$ prevented the corrosion of these metal oxides. Improved suppression of HER was observed with the addition of these layers, as can be seen in Figure 2a for SiO$_2$. In this type of structure, tunneling rate is controlled primarily through the thickness of Al$_2$O$_3$ or SiO$_2$. However, thickness of the HfO$_2$ layer also impacts current density through the barrier, as seen in Figure 2b.
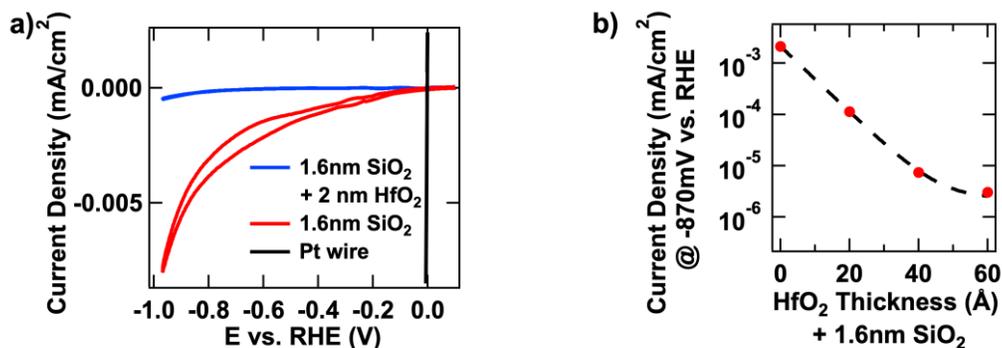

Figure 2: (a) Cyclic voltammetry for different electrodes. Pt wire reference is shown, in addition to 1.6 nm SiO$_2$ and 2 nm ALD HfO$_2$ on-top of 1.6 nm SiO$_2$. (b) Current dependence on ALD HfO$_2$ thickness.

Engineering of the catalyst-insulator interface for the full catalyst-insulator-metal device was concurrently investigated with HfO$_2$ performance. One key problem was adhesion of the Re nanoparticle catalyst layer to the underlying HfO$_2$. Several strategies were explored for improving catalyst adhesion to the insulator surface. Simple solvent rinse tests were used to evaluate adhesion, where Re content was measured either via a thickness change (as measured with ellipsometry) or as a change in relative atomic percent (as measured with x-ray photoelectron spectroscopy [XPS]).

Annealing the device after catalyst deposition showed little promise for preventing its loss. Both room temperature and baked at 150 °C HfO_2 lost all Re after a water rinse, as seen in Table I. Increasing temperature beyond this resulted in massive Re loss during the anneal stage, which was attributed to the formation and subsequent sublimation of rhenium oxides.

Temperature (°C)	Time (minutes)	Re Thickness (Å)	
		Post-Anneal	Post-Rinse
25	N/A	7.5	0
150	60	4	0
200	60	0.5	N/A
300	60	0	N/A

Table I: Re layer thickness as measured by ellipsometry under various annealing conditions, before and after rinsing with water.

Another strategy for improving the catalyst-insulator interface was the addition of a thin Hf "sticking" layer to the surface of the insulator; this was deposited by sputtering, and immediately followed by catalyst deposition without breaking vacuum. This was concurrently investigated with in-situ biasing to increase the landing velocity of the nanoparticles. Table II shows the results of these experiments. Incorporating these strategies substantially improved the adhesion of Re to a HfO_2-based device; whereas previously all Re was lost after rinsing, half or more remained when incorporating a sticking layer or sticking layer with bias.

Bias	Hf Deposition Time			
	10 sec		20 sec	
	[Re]/[Re+Hf] Pre-Rinse	[Re]/[Re+Hf] Post-Rinse	[Re]/[Re+Hf] Pre-Rinse	[Re]/[Re+Hf] Post-Rinse
0 kV	N/A	N/A	45.5 %	26.5 %
1 kV	20.0 %		36.0 %	14.5 %
5 kV	10.5 %	7.5 %	7.5 %	7.5 %

Table II: Re adhesion study with added Hf sticking layer and biased deposition of Re nanoparticles. Amount of Re on surface is determined by calculating the relative ratios of Re and Hf as measured by XPS.

Although the HfO2 capping layer is effective in preventing corrosion of the barrier material, it interferes with directly exploring the tunneling behavior of the other candidate barrier materials.. ALD Al_2O_3 was chosen for further investigation to determine if there existed conditions under which corrosion would be mitigated. Thus, we evaluated the stability of the Re nanoparticles on Al_2O_3 under several solvent systems, including propylene carbonate (PC), a solution of 50% ethylene glycol (EG) in water, ethanol, and

tetrahydrofuran (THF). Although the 50% ethylene glycol solution showed the lowest catalyst loss (Figure 3), propylene carbonate was ultimately selected as it would allow for more options in organic redox probes necessary for evaluating the electrical properties of the barrier.
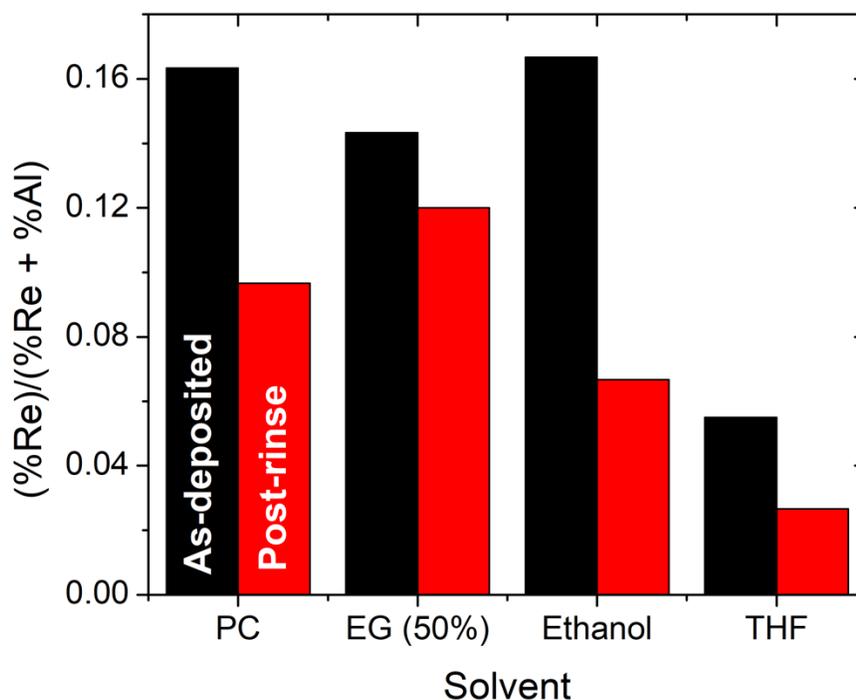

Figure 3: Adhesion study of Re on Al$_2$O$_3$ with various solvents. Amount of Re on surface is determined by calculating the relative ratios of Re and Al as measured by XPS.

The stability of Al$_2$O$_3$ against corrosion was investigated by cycling in PBS at pH=7. This resulted in slow corrosion, leading to increasing current with time. Stability of ALD Al$_2$O$_3$ was greatly enhanced in non-aqueous electrolyte. In this work, we used propylene carbonate as the solvent and tetrabutylammonium triflate as the supporting electrolyte. Redox active species, NiCp$_2$ and FeCp$_2$ were used to probe electron/hole transfer through the barrier. Upon oxidative scans, Al$_2$O$_3$ deposited on gold was stable, as seen in Figure 4a. The oxidative current is attributed to oxidation of NiCp$_2$/FeCp$_2$ in solution, while reduction current is attributed to reduction of the cation, tetrabutyammonium (TBA). The current-voltage behavior was stable over time, and actually resulted in a slight decrease in current with time. However, upon scanning to more reducing potentials, degradation of the film was observed (Figure 4b). In addition to the current increasing with the number of scans, the oxidation of NiCp$_2$ near 0V became visible, indicating breakthrough to the underlying gold substrate. In addition, the bandgap of Al$_2$O$_3$ should be >6V. It is apparent in Figure 6 that the passivated window for a 2nm film is <3V wide and indicates that conduction is occurring through mid-band gap states.
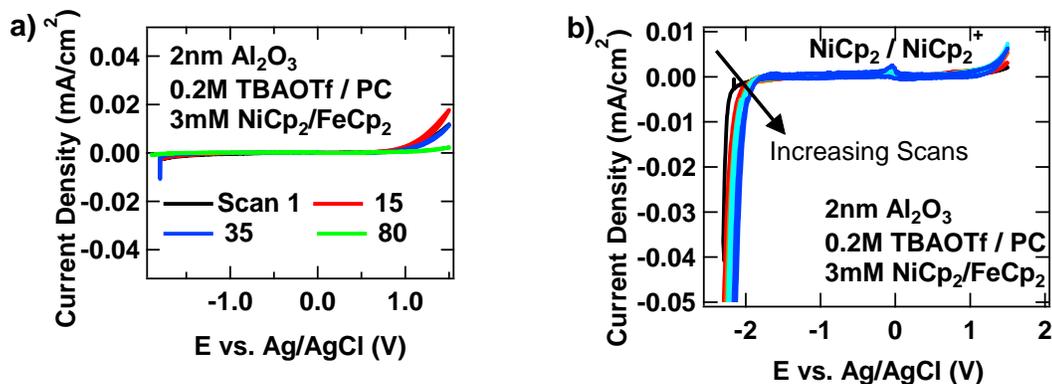
Figure 4:(a) Cyclic voltammetry of 2nm ALD Al_2O_3 on gold substrate in 0.2M tetrabutylammonium triflate (TBAOTf)/ Propylene Carbonate (PC) and 3mM $NiCp_2$ and $FeCp_2$, showing the range of stability. (b) Cyclic voltammetry when more reducing potentials applied to the same sample. Degradation of film is observed, with appearance of $NiCp_2$ oxidation observed near 0V and increasing current densities with increasing scan number.

Conclusions

The goal of this research was to develop a metal-insulator-catalyst device that improved the selectivity of the NRR by depriving the HER of electrons via a tunneling junction. This work highlighted the challenges of integrating and optimizing several components into a fully functional, ammonia-producing device. Engineering remains a challenge on top of the already difficult scientific problem of NRR.

During the course of this program, we demonstrated progress in some of the key building blocks for achieving our larger goal. We successfully showed that HER could be dampened by tuning the thickness of an insulator. We demonstrated some strategies for improving often poor adhesion between a catalyst and its underlying surface in an electrochemical system. These pieces fit into the larger toolbox of strategies needed to tackle the challenging problems in electrochemistry. The approach of limiting electron availability in a metal-insulator-catalyst device could also prove useful in CO_2 electrochemistry. Like with ammonia and the NRR, selectivity for the CO_2 reduction reaction is in general poor and struggles to compete with the HER. Development of an efficient way to recycle atmospheric CO_2 into useful chemical compounds could prove invaluable in closing the carbon cycle.

Though a viable, low-energy alternative for Haber-Bosch is still not here, work remains intense in developing devices for electrochemical ammonia production. Such a device has the potential for huge impact in reduction of GHG emissions on a global scale by cutting into the massive 2% share of global energy consumption that ammonia claims. A competitive process for production electrochemically has the potential to completely change the game on ammonia, allowing for decentralized production in renewable-powered plants. The replacement for Haber-Bosch could ultimately prove as revolutionary to the battle against GHG emissions as its predecessor did to food production a hundred years ago.

References

1. Erisman, J.W., Sutton, M. A., Galloway, J., Klimont, Z., and Winiwarter, W. How a century of ammonia synthesis changed the world, *Nature Geoscience*, **1**, 636-639 (2008). DOI: 10.1038/ngeo325
2. Service, R. F. New recipe produces ammonia from air, water, and sunlight, *Science*, **345**:6197, 610 (2014). DOI: 10.1126/science.345.6197.610
3. Ali, M., Zhou, F., Chen, K., Kotzur, C., Xiao, C., Bourgeois, L., Zhang, X., and MacFarlane, D.R. Nanostructured photoelectrochemical solar cell for nitrogen reduction using plasmon-enhanced black silicon, *Nature Communications*, **7**, 11335 (2016). DOI: 10.1038/ncomms11335
4. Andersen, S.Z. *et al*. A rigorous electrochemical ammonia synthesis protocol with quantitative isotope measurements, *Nature*, **1476**:4687, 1260 (2019). DOI: 10.1038/s41586-019-1260-x
5. Zhou, F., Azofra, L.M., Ali, M., Kar, M., Simonov, A.N., McDOnnell-Worth, C., Sun, C., Zhang, X., and MacFarlane, D.R. Electro-synthesis of ammonia from nitrogen at ambient temperature and pressure in ionic liquids, *Energy & Environmental Science,* **10**, 2516-2520 (2017). DOI: 10.1039/C7EE02716H
6. McEnaney, J.M., Singh, A.R., Schwalbe, J.A., Kibsgaard, J., Lin, J.C., Cargnello, M., Jaramillo, T.F., and Norskov, J.K. Ammonia synthesis from N2 and H2O using a lithium cycling electrification strategy at atmospheric pressure, *Energy & Environmental Science,* **10,** 1621-1630 (2017). DOI: 10.1039/C7EE01126A
7. Lazouksi, N., Schiffer, Z.J., Williams, K., and Manthiram, K. Understanding Continuous Lithium-Mediated Electrochemical Nitrogen Reduction, *Joule*, **3**:4, 1127-1139 (2019). DOI: 10.1016/j.joule.2019.02.003
8. Tsuneto, A., Kudo, A., and Sakata, T. Lithium-mediated electrochemical reduction of high pressure N2 to NH3, *Journal of Electroanalytical Chemistry*, **367**:1-2, 183-188 (1994). DOI: 10.1016/0022-0728(93)03025-K
9. Oshikiri, T., Ueno, K., and Misawa, H. Selective Dinitrogen Conversion to Ammonia Using Water and Visible Light through Plasmon-induced Charge Separation, *Angewandte Chemie International Edition*, **55**:12, 3942-3946 (2016). DOI: 10.1002/anie.201511189

Contacts

Stacey F. Bent: sbent@stanford.edu
Bruce Clemens: bmc@stanford.edu
Jon Baker: jgbaker@stanford.edu
Melissa Wette: mwette@stanford.edu